A Cutoff Invariant Two-Scale Model in Electromagnetic Scattering From Sea Surfaces

Gabriel Soriano and Charles-Antoine Guérin

***Abstract*—The two-scale model (TSM) is one of the most frequently employed approaches in scattering from multiscale surfaces such as ocean surfaces. It consists of combining geometrical optics (GO) with the small-perturbation model (SPM) to be able to cope with both the small- and large-scale components of the surface. However, well-known shortcomings of this method are the arbitrariness of the dividing scale and the sensitivity of the scattering cross section to the choice of this parameter. We propose to replace SPM with the first-order small-slope approximation (SSA1) to treat the small-scale roughness and derive the formulas for the corresponding TSM, referred to as GO-SSA. We show that GO-SSA is robust to the choice of the frequency cutoff and give a numerical illustration for the sea surface.**

***Index Terms*—Ocean scattering, small slope approximation (SSA), two-scale model (TSM).**

I. Introduction

THE composite-surface model, or two-scale model (TSM) [1]–[4], is currently the most employed for calculation of ocean-surface scattering. In this model, the surface is considered as a superposition of long waves and short ripples. The contribution of each kind of roughness to the scattering process is then treated differently. The formulation of the TSM varies with authors and applications: radar backscattering coefficient, surface brightness temperature, etc.

In its simplest expression, the TSM combines geometrical optics (GO) for long waves and the small-perturbation method at first order (SPM1) for short waves. In terms of scattering cross section, it can be symbolically summarized as follows:

$$\text{GO} - \text{SPM} = \text{GO} + \text{SPM1} * (\text{pdf slopes}). \tag{1}$$

The TSM relies on a cutoff parameter, which divides the elevation spectrum into small- and large-scale waves. In the derivation of this model, the cutoff frequency is chosen large enough to ensure that the exponential quantities involving the small-scale wave correlation function can be linearized (see, e.g., the discussion in [5]). However, the applicability of the GO to the remaining long-wave components is not guaranteed, as there is, in general, no common regime for Bragg and GO scattering from ocean surfaces. Therefore, some authors recommend that values of the cutoff be obtained by comparison with experimental data or numerical simulations [6], [7]. This value will change with the electromagnetic (EM) frequency but also with the incidence angle and the wind condition. Another weakness of (1) is that GO-SPM is at least equal to the GO and that small-scale roughness has no impact on this term. Since Wright in 1968 [1], several advanced methods have been published that can theoretically cope with the ocean-surface scattering at any frequency (see, e.g., [8], for a review). However, these methods are often complex, and their application to multiscale surfaces, such as the ocean, can quickly become tricky and computationally intensive. The aim of this letter is to show that, with minimum change, the TSM can be made more reliable in the sense that its dependence on the cutoff is relegated to a position of secondary importance.

The main idea is that SPM1 has too tight of a validity domain and should be replaced with the small-slope approximation [9], [10] at first order (SSA1). This method has a wider validity domain than SPM1 while being of the same complexity as a mere Kirchhoff approximation. Furthermore, it has been shown [11] to be very accurate on the ocean elevation spectrum as long as the lowest frequency components of the spectrum are truncated. However, the main weakness of SSA1 is its inconsistency with GO for large scales, which makes it unable to cope with the longest ocean waves (except at low EM frequency and/or low wind speed). This is why SSA1 cannot be used alone to treat the whole ocean surface and has to be incorporated in a TSM. Nevertheless, its domain of validity is sufficiently large to allow a displacement of the cutoff toward nonresonant frequencies in the validity domain of GO. Therefore, we propose to combine the GO for long waves and SSA1 for short waves in an improved TSM, called GO-SSA. In Section II, a complete development of the GO-SSA is given. For the convenience of the practitioner, we provide explicit formulas of the GO-SSA model in Section III. In Section IV, the GO-SSA applied to the unified directional ocean spectrum [12] is proved to be quasi independent of the cutoff. A numerical illustration is given for both the monostatic and the bistatic case.

II. Formulation of the Model

We consider a rough surface Σ, centered about the horizontal (x, y) plane separating vacuum (upper medium) from a homogeneous medium with complex relative permittivity ε_r (lower medium). The surface is illuminated from above by a unitary plane wave $e^{i\boldsymbol{K_0}\cdot\boldsymbol{R}}$ with wave vector $\boldsymbol{K}_0$, where $\boldsymbol{R} = (x, y, z)$ is the 3-D position vector. The scattered waves in the upper medium are labeled by their wave vector $\boldsymbol{K}$. The scattering tensor $\mathbb{S}$ associated with the surface is defined by

$$\boldsymbol{E}_{\text{s}} = -i\frac{e^{iKR}}{R}\mathbb{S}(\boldsymbol{K}, \boldsymbol{K}_0)\boldsymbol{E}_0 \tag{2}$$

Manuscript received November 13, 2006; revised September 18, 2007.

G. Soriano is with the Université Paul Cezanne, Institut Fresnel UMR CNRS 6133, 13397 Marseille Cedex 20, France.

C.-A. Guérin was with the Université Paul Cezanne, Institut Fresnel UMR CNRS 6133, 13397 Marseille Cedex 20, France. He is now with the Laboratiore de Sondages Electromagnétiques de l'Environnement Terrestre, Université du Sud-Toulon Var, 83597 La Garde, France.

Digital Object Identifier 10.1109/LGRS.2008.915746

where $\boldsymbol{E}_{\mathrm{s}}$ is scattered far field at distance R and in direction $\boldsymbol{K}$ and $\boldsymbol{E}_0$ is the incident polarization. As usual, in the TSM, the surface elevation is decomposed into small- and large-scale components. We assimilate the large-scale component to a succession of adjoining randomly tilted plane facets with the same projected area A. We denote $\boldsymbol{n_j}$ as the unit normal vector of the $\boldsymbol{j}$th facet and $\boldsymbol{R_j}$ as the position vector of its center. The small-scale component h_{s} is a stationary centered Gaussian random process with rms deviation $\sigma_{\mathrm{s}} = \langle h_{\mathrm{s}}^2 \rangle^{1/2}$, superimposed on the facets along their normal direction. Hence, the surface is described by the position vector

$$\boldsymbol{R}_{|\Sigma} = \tilde{\boldsymbol{r}} + h_{\mathrm{s}}(\tilde{\boldsymbol{r}})\boldsymbol{n} \tag{3}$$

where $\tilde{\boldsymbol{r}}$ is a vector along the large-scale facet, $\boldsymbol{n}$ is the local normal vector, and h_{s} is understood as a function of two coordinates in the framework of this facet. We suppose that there is no correlation between the successive facet slopes nor between the small- and large-scale processes. Our analysis relies on the fundamental assumption that the rough facets scatter coherently yet without coupling. We therefore write

$$\mathbb{S}(\boldsymbol{K}, \boldsymbol{K}_0) = \sum_{\boldsymbol{j} \in \mathbb{Z}^2} \mathbb{S}_{\boldsymbol{j}} \tag{4}$$

with the convention that $\mathbb{S}_{\boldsymbol{j}}$ is the scattering amplitude of the $\boldsymbol{j}$th facet illuminated by a truncated plane wave $e^{i\boldsymbol{K_0}\cdot\boldsymbol{R}}\Pi_A(\boldsymbol{R} - \boldsymbol{R}_j)$. Here, the cutoff function Π_A delimits the region of space whose vertical projection falls within the area A: $\Pi_A(x, y, z)$=1 if $(x, y) \in A$, else $\Pi_A(x, y, z) = 0$. The scattering amplitude of each rough facet will be calculated by means of SSA1, evaluated in its local framework. We now proceed with the evaluation of the coherent and incoherent cross sections, which are related to the mean and fluctuation of the scattering amplitude over the roughness process. We denote by $\langle\cdot\rangle_{\mathrm{s}}$, $\langle\cdot\rangle_{\mathrm{L}}$, and $\langle\cdot\rangle_{\mathrm{s,L}}$ the ensemble average over small-, large-, and composite scales, respectively. At this stage, it is convenient to introduce the Ewald vector $\boldsymbol{Q} = \boldsymbol{K} - \boldsymbol{K}_0$. We denote $q_\perp^{\boldsymbol{j}} = \boldsymbol{Q}\cdot\boldsymbol{n_j}$ and $\boldsymbol{q}_\parallel^{\boldsymbol{j}} = \boldsymbol{Q} - q_\perp^{\boldsymbol{j}}\boldsymbol{n}_j$ as its normal and in-plane component, respectively, with respect to a facet with normal $\boldsymbol{n_j}$. The scattering amplitude of the $\boldsymbol{j}$th facet under SSA1 is given by

$$\mathbb{S}_{\boldsymbol{j}} = \frac{2\pi}{q_\perp^{\boldsymbol{j}}} e^{-i\boldsymbol{Q}\cdot R_j}\mathbb{B}(\boldsymbol{K}; \boldsymbol{K}_0; \boldsymbol{n}_j) \times \frac{1}{4\pi^2}\int d\tilde{\boldsymbol{r}}\Pi_A(\tilde{\boldsymbol{r}})e^{-i\boldsymbol{Q}\cdot[\tilde{\boldsymbol{r}} + h(\tilde{\boldsymbol{r}})\boldsymbol{n}_j]} \tag{5}$$

where the vector $\tilde{\boldsymbol{r}}$ runs over the facet and $\mathbb{B}(\boldsymbol{K}; \boldsymbol{K}_0; \boldsymbol{n}_j)$ is the Bragg scattering tensor associated with the tilted plane. Performing an ensemble average over small scales, we obtain the coherent component of each facet

$$\langle\mathbb{S}_{\boldsymbol{j}}\rangle_{\mathrm{s}} = \frac{2\pi}{q_\perp^{\boldsymbol{j}}} e^{-i\boldsymbol{Q}\cdot\boldsymbol{R}_j}\mathbb{B}(\boldsymbol{K}; \boldsymbol{K}_0; \boldsymbol{n}_j)e^{-\frac{1}{2}\left(q_\perp^{\boldsymbol{j}}\sigma_{\mathrm{s}}\right)^2} \times \frac{1}{4\pi^2}\int d\tilde{\boldsymbol{r}}\Pi_A(\tilde{\boldsymbol{r}})e^{-i\boldsymbol{q}_\parallel^{\boldsymbol{j}}\cdot\tilde{\boldsymbol{r}}}. \tag{6}$$

The integration variable can be converted to a horizontal variable $\boldsymbol{r}$ through the correspondence

$$d\tilde{\boldsymbol{r}} \to \left(1 + s_j^2\right)^{1/2} d\boldsymbol{r} \quad \Pi_A(\tilde{\boldsymbol{r}}) \to \Pi_A(\boldsymbol{r}) \quad \boldsymbol{q}_\parallel^{\boldsymbol{j}}\cdot\tilde{\boldsymbol{r}} \to \boldsymbol{q}_H + \boldsymbol{q}_z\boldsymbol{s}_j\cdot\boldsymbol{r}$$

where $q_z = \boldsymbol{Q}\cdot\widehat{z}$ and $\boldsymbol{q}_H = \boldsymbol{Q} - q_z\widehat{z}$ designate the vertical and horizontal components of the Ewald vector, respectively. Hence

$$\langle\mathbb{S}_{\boldsymbol{j}}\rangle_{\mathrm{s}} = \frac{2\pi}{q_\perp^{\boldsymbol{j}}} e^{-i\boldsymbol{Q}\cdot R_j}\mathbb{B}(\boldsymbol{K}; \boldsymbol{K}_0; \boldsymbol{n}_j)e^{-\frac{1}{2}\left(q_\perp^{\boldsymbol{j}}\sigma_{\mathrm{s}}\right)^2} \times \left(1 + s_j^2\right)^{1/2}\widehat{\Pi}_A(\boldsymbol{q}_H + q_z\boldsymbol{s}_j) \tag{7}$$

where $\widehat{\Pi}_A$ is the 2-D Fourier transform of Π_A

$$\widehat{\Pi}_A(\boldsymbol{\xi}) = \frac{1}{4\pi^2}\int_{\mathbb{R}^2} d\boldsymbol{r}e^{-i\boldsymbol{\xi}\cdot r}\Pi_A(\boldsymbol{r}). \tag{8}$$

Typically, the facet is much larger than the incident wavelength so that the function $\widehat{\Pi}_A$ is sharply peaked around the local specular direction. Hence, the involved quantities must be evaluated at the specular slope

$$\boldsymbol{s}_j \to -\boldsymbol{q}_H/q_z \quad \boldsymbol{n}_j \to \widehat{\boldsymbol{Q}} := \frac{\boldsymbol{Q}}{Q}. \tag{9}$$

The Bragg scattering tensor in the local specular direction can be expressed [8] through the Fresnel reflection operator (see Section III for explicit definitions)

$$\mathbb{B}(\boldsymbol{K}; \boldsymbol{K}_0; \widehat{\boldsymbol{Q}}) = \frac{Q^2}{2}\mathbb{R}\left(\frac{\boldsymbol{K} + \boldsymbol{K}_0}{2}; \widehat{\boldsymbol{Q}}\right). \tag{10}$$

Altogether, this gives the coherent contribution of a single facet

$$\langle\mathbb{S}_{\boldsymbol{j}}\rangle_{\mathrm{s}} = e^{-i\boldsymbol{Q}\cdot R_j}\mathbb{V}\widehat{\Pi}_A(\boldsymbol{q}_H + q_z\boldsymbol{s}_j) \tag{11}$$

where we have introduced the tensor

$$\mathbb{V} = 2\pi e^{-(Q\sigma_{\mathrm{s}})^2/2}\frac{Q^2}{2q_z}\mathbb{R}\left(\frac{\boldsymbol{K} + \boldsymbol{K}_0}{2}; \widehat{\boldsymbol{Q}}\right). \tag{12}$$

Further averaging over the large scales under the assumption that the facet altitudes $H_{\boldsymbol{j}} = \boldsymbol{R_j}\cdot\widehat{z}$ and slopes $\boldsymbol{s_j}$ are Gaussian and independent random variables leads to

$$\langle\mathbb{S}_j\rangle_{\mathrm{s,L}} = \mathbb{V}e^{-(q_z\sigma_{\mathrm{L}})^2/2}e^{-i\boldsymbol{q}_H\cdot r_j}\left[\widehat{\Pi}_A(-q_z\cdot) * P\right](-\boldsymbol{q}_H/q_z) \tag{13}$$

where $\sigma_{\mathrm{L}} = \langle H_j^2\rangle_{\mathrm{L}}$ is the large-scale rms height, P is the pdf of slopes, and the asterisk stands for the convolution. The incoherent scattering cross section is obtained by normalizing the scattered intensity by an increasing illuminated area. It can therefore be written as

$$\sigma(\boldsymbol{K}, \boldsymbol{K}_0) = \lim_{N\to\infty}\frac{1}{NA}\sigma_N(\boldsymbol{K}, \boldsymbol{K}_0) \tag{14}$$

where σ_N is the intensity produced by the illumination of N facets, each of which has projected area A

$$\sigma_N(\boldsymbol{K}, \boldsymbol{K}_0) = \sum_{|\boldsymbol{j}|,|\boldsymbol{j}'|\le N}\left[\left\langle S_{\boldsymbol{j}}S_{\boldsymbol{j}'}^*\right\rangle_{\mathrm{s,L}} - \langle S_{\boldsymbol{j}}\rangle_{\mathrm{s,L}}\left\langle S_{\boldsymbol{j}'}^*\right\rangle_{\mathrm{s,L}}\right]. \tag{15}$$

Here, $S_{\boldsymbol{j}}$ refers to any of the four components of the scattering tensor in a polarization basis. Now, we can decompose each elementary scattering amplitude into a mean and fluctuating part with respect to the small-scale average

$$S_{\boldsymbol{j}} = \langle S_{\boldsymbol{j}} \rangle_{\mathrm{s}} + \delta S_{\boldsymbol{j}}. \tag{16}$$

The assumption that the facets' slopes are independent implies that both the mean and fluctuating part of the local scattering amplitudes are uncorrelated from one facet to another, leading to

$$\sigma(\boldsymbol{K}, \boldsymbol{K}_0) = \frac{1}{A}\left(\left\langle \left\langle |\delta S_{\boldsymbol{j}}|^2 \right\rangle_{\mathrm{s}} \right\rangle_{\mathrm{L}} + \left\langle |\langle S_{\boldsymbol{j}} \rangle_{\mathrm{s}}|^2 \right\rangle_{\mathrm{L}} - |\langle S_{\boldsymbol{j}} \rangle_{\mathrm{s,L}}|^2 \right). \tag{17}$$

The first term is the incoherent cross section of SSA1 applied to small scales in their local framework and averaged over large-scale slopes

$$\frac{1}{A}\left\langle \left\langle |\delta S_{\boldsymbol{j}}|^2 \right\rangle_{\mathrm{s}} \right\rangle_{\mathrm{L}} = \langle \sigma_{\mathrm{SSA1}}(\boldsymbol{K}, \boldsymbol{K}_0; \boldsymbol{n}) \rangle_{\mathrm{L}}\,. \tag{18}$$

The remaining contribution in (17) is the variance over large scales, $\mathrm{Var}(\langle S_{\boldsymbol{j}} \rangle_{\mathrm{s}})\rangle_{\mathrm{L}}$, of the small-scale coherent field, normalized by the area

$$\frac{\mathrm{Var}\left(\langle S_{\boldsymbol{j}} \rangle_{\mathrm{s}}\right)\rangle_{\mathrm{L}}}{A} = \frac{|V|^2}{A}\Bigg(\left| \widehat{\Pi}_A(-q_z \cdot) \right|^2 * P - e^{-(q_z \sigma_{\mathrm{L}})^2} \left| \widehat{\Pi}_A(-q_z \cdot) * P \right|^2 \Bigg)(-\boldsymbol{q}_H/q_z). \tag{19}$$

Here, V stands for any component of $\mathbb{V}$ in the polarization basis. When the facet area A is much larger than the EM wavelength, we have $\widehat{\Pi}_A(\boldsymbol{\xi}) \sim \delta(\boldsymbol{\xi})$ and $|\widehat{\Pi}_A(\boldsymbol{\xi})|^2 \sim A/(4\pi^2)\delta(\boldsymbol{\xi})$. On the other hand, the large-scale rms height σ_{L} and slope s_{L} tend to zero as the facet size is increased, since there are fewer and fewer scales beyond this dividing scale. Hence, we have also $P(\boldsymbol{\xi}) \to \delta(\boldsymbol{\xi})$ in the limit $A \to \infty$, and the term (19) must be handled with caution. If the support of the function P is much smaller than that of $\widehat{\Pi}_A$ (i.e., $q_z^2 A s_{\mathrm{L}}^2 \ll 1$), then we can first replace P with a delta function in the convolution to obtain

$$\frac{\mathrm{Var}\left(\langle S_{\boldsymbol{j}} \rangle_{\mathrm{s}}\right)\rangle_{\mathrm{L}}}{A} = \frac{|V|^2}{4\pi^2}\delta(\boldsymbol{q}_H)\left(1 - e^{-(q_z \sigma_{\mathrm{L}})^2}\right). \tag{20}$$

If on the contrary $q_z^2 A s_{\mathrm{L}}^2 \gg 1$, then it is $\widehat{\Pi}_A$ that plays the role of a delta function in the convolution, and we have

$$\frac{\mathrm{Var}\left(\langle S_{\boldsymbol{j}} \rangle_{\mathrm{s}}\right)\rangle_{\mathrm{L}}}{A} \simeq \frac{|V|^2}{4\pi^2 q_z^2} P(-\boldsymbol{q}_H/q_z). \tag{21}$$

Note that the contribution arising from the latter term in (19) is negligible in that case, since for Gaussian pdf, it is of the order $P^2/(q_z^2 A) \sim P/(q_z^2 A s_{\mathrm{L}}^2)$. Since σ_{L} and s_{L} have the same monotonic behavior with respect to the facet size, we chose to condense (20) and (21) into a single approximate form

$$\frac{\mathrm{Var}\left(\langle S_{\boldsymbol{j}} \rangle_{\mathrm{s}}\right)\rangle_{\mathrm{L}}}{A} = \frac{|V|^2}{4\pi^2 q_z^2} P(-\boldsymbol{q}_H/q_z)\left[1 - e^{-(q_z \sigma_{\mathrm{L}})^2}\right]. \tag{22}$$

Altogether, the two-scale incoherent cross section can be written

$$\sigma(\boldsymbol{K}, \boldsymbol{K}_0) = \langle \sigma_{\mathrm{SSA1}}(\boldsymbol{K}, \boldsymbol{K}_0; \boldsymbol{n}) \rangle_{\mathrm{L}} + \left(1 - e^{-(q_z \sigma_{\mathrm{L}})^2}\right) \times e^{-Q^2 \sigma_{\mathrm{s}}^2} \left| R\left(\frac{\boldsymbol{K} + \boldsymbol{K}_0}{2}; \widehat{\boldsymbol{Q}} \right) \right|^2 \frac{Q^4}{4 q_z^4} P(-\boldsymbol{q}_H/q_z) \tag{23}$$

which holds for any of the four components of the involved quantities in a polarization basis. The first term is the orientation average over large-scale slopes of the local SSA1 cross section applied to the small scale. The second term is identified as the usual GO cross section of large scales damped by an exponential attenuation factor due to the small-scale coherent field. The main result of this paper can thus be summed up in the symbolic equation as follows:

$$\mathrm{GO-SSA} = \mathrm{GO} \times e^{-Q^2 \sigma_{\mathrm{s}}^2}\left[1 - e^{-(q_z \sigma_{\mathrm{L}})^2}\right] + \mathrm{SSA1} * (\text{pdf slopes}). \tag{24}$$

A consistency test on this formula can be performed by inspecting the limiting cases. GO is plainly recovered in the absence of small scale ($\sigma_{\mathrm{s}} = 0$) and for large Rayleigh parameter ($q_z \sigma_{\mathrm{L}} \gg 1$). If the large-scale components are set to zero, the pdf of slope becomes a delta function, and the incoherent cross section reduces to that of SSA1. The qualitative behavior of each of the terms as the cutoff frequency ($K_{\mathrm{c}} \sim A^{-1/2}$) is varied makes GO-SSA robust to the latter. Indeed, moving K_{c} toward high frequencies diminishes the small-scale rms and the SSA1 incoherent cross section. This is, however, compensated by the increase of the damping exponential factor due to small-scale roughness.

Note that this factor has already appeared in the literature, in earlier attempts to modify the TSM, by treating the small-scale part with a different theory from SPM, essentially the Kirchhoff approximation [13]–[15].

III. Explicit Formulas for the GO-SSA Model

For the convenience of the practitioner, we provide explicit formulas of the GO-SSA model in the standard polarization basis. To avoid tedious use of change of basis matrices, it is convenient to express the SSA1 scattering amplitude in a dyadic form, which is not bound to the choice of a reference framework. The Bragg scattering matrix involved in SSA1 can be written as per [8], [16]

$$\mathbb{B}(\boldsymbol{K}; \boldsymbol{K}_0; \boldsymbol{n}) = -\frac{\varepsilon - 1}{2} K^2 \left[1 - \widehat{\boldsymbol{K}}\widehat{\boldsymbol{K}} + \mathbb{R}(\boldsymbol{K}; \boldsymbol{n})\right] \times \left[1 + \left(\frac{1}{\varepsilon} - 1\right)\boldsymbol{n}\boldsymbol{n}\right]\left[1 - \widehat{\boldsymbol{K}}_0\widehat{\boldsymbol{K}}_0 + \mathbb{R}(\boldsymbol{K}_0; \boldsymbol{n})\right]$$

with $\widehat{\boldsymbol{K}} = \boldsymbol{K}/K$ and $\widehat{\boldsymbol{K}}_0 = \boldsymbol{K}_0/K$. The involved Fresnel reflection operator is given by

$$\mathbb{R}(\boldsymbol{K}; \boldsymbol{n}) = \sum_{i=1,2} r_i(K_\perp) \boldsymbol{p}_i^+(\boldsymbol{K}; \boldsymbol{n}) \boldsymbol{p}_i^-(\boldsymbol{K}; \boldsymbol{n}) \tag{25}$$

where $K_\perp = |\boldsymbol{K} \cdot \boldsymbol{n}|$ is the absolute normal component of the wave vector and r_1 and r_2 are the Fresnel reflection coefficients

in vertical and horizontal polarization, respectively, evaluated at the local angle. We have denoted $\boldsymbol{p}_i^{\pm}$ as the vectors forming the canonical polarization basis in the framework of the tilted plane for upgoing $(\boldsymbol{p}_i^{+})$ and downgoing $(\boldsymbol{p}_i^{-})$ plane waves. They are given by

$$\boldsymbol{p}_2^{\pm}(\boldsymbol{K};\boldsymbol{n}) = \frac{\boldsymbol{n}\times\boldsymbol{K}}{\|\boldsymbol{n}\times\boldsymbol{K}\|}$$

$$\boldsymbol{p}_1^{\pm}(\boldsymbol{K};\boldsymbol{n}) = \frac{1}{K}(\boldsymbol{K}_{\parallel} \pm K_{\perp}\boldsymbol{n})\times\boldsymbol{p}_2^{\pm}(\boldsymbol{K};\boldsymbol{n})$$

with $\boldsymbol{K}_{\parallel} = \boldsymbol{K} - \boldsymbol{K}\cdot\boldsymbol{n}\boldsymbol{n}$. Each of the components of the incoherent SSA1 cross section, $\langle\sigma_{\mathrm{SSA1}}^{ji}(\boldsymbol{K},\boldsymbol{K}_0;\boldsymbol{n})\rangle_{\mathrm{L}}$, is obtained through

$$\left\langle \left|\boldsymbol{p}_j^{+}(\boldsymbol{K};\widehat{z})\mathbb{B}(\boldsymbol{K};\boldsymbol{K}_0;\boldsymbol{n})\boldsymbol{p}_i^{-}(\boldsymbol{K}_0;\widehat{z})\right|^2 \mathcal{L}(\boldsymbol{Q};\boldsymbol{n})\right\rangle_{\mathrm{L}} \quad (26)$$

where i and j denote the incident and scattered polarization, respectively. Here, the function $\mathcal{L}$ is given by

$$\mathcal{L}(\boldsymbol{Q};\boldsymbol{n}) = \frac{1}{4\pi^2}e^{-q_\perp^2\sigma_{\mathrm{s}}^2}\int\limits_{\mathbb{R}^2} d\boldsymbol{r}e^{-i\boldsymbol{q}_{\parallel}\cdot\boldsymbol{r}}\left[e^{q_\perp^2 C(\boldsymbol{r})}-1\right] \quad (27)$$

where $C(\boldsymbol{r}) = \langle h(0)h(\boldsymbol{r})\rangle_{\mathrm{s}}$ is the correlation function of the small-scale process. In the literature, the Fourier transform of the ocean correlation, the elevation spectrum

$$\Psi(k,\varphi) = \frac{B(k)}{2\pi k^4}\left(1+\Delta(k)\cos 2\varphi\right) \quad (28)$$

is generally expressed in polar coordinates (k,φ), $\varphi = 0$ being the upwind direction, with the help of the omnidirectional curvature spectrum $B(k)$ and the spreading function $\Delta(k)$ [12]. Consequently, the small-scale correlation in polar coordinates can be written as $C(r,\theta) = C_0(r) + C_2(r)\cos 2\theta$ with

$$C_0(r) = \int\limits_{k>K_{\mathrm{c}}} \frac{B(k)}{k^3}J_0(kr)dk$$

$$C_2(r) = -\int\limits_{k>K_{\mathrm{c}}} \frac{B(k)\Delta(k)}{k^3}J_2(kr)dk. \quad (29)$$

Under the assumption that the small-scale roughness is weakly anisotropic: $K^2C_2 \ll 1$, integral (27) is also a sum $\mathcal{L} = \mathcal{L}_0 + \mathcal{L}_2\cos 2\varphi$ with

$$\mathcal{L}_0 = \frac{e^{-q_\perp^2\sigma_{\mathrm{s}}^2}}{2\pi}\int\limits_0^{\infty}\left[e^{q_\perp^2 C_0(r)}-1\right]J_0(q_{\parallel}r)rdr$$

$$\mathcal{L}_2 = -q_\perp^2\frac{e^{-q_\perp^2\sigma_{\mathrm{s}}^2}}{2\pi}\int\limits_0^{\infty} C_2(r)e^{q_\perp^2 C_0(r)}J_2(q_{\parallel}r)rdr \quad (30)$$

and $\boldsymbol{q}_{\parallel} = (q_{\parallel},\varphi)$ in polar coordinates.

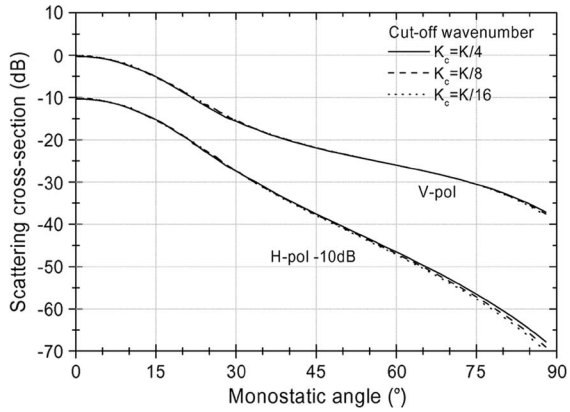

Fig. 1. Ocean backscattering cross section at Ku-band ($f = 14.6$ GHz) predicted by the GO-SSA versus the monostatic incidence angle, along wind, for a wind speed of 15 m/s and for three values of the cutoff wavenumber. For clarity, a 10-dB attenuation has been applied to the horizontally polarized component.

Numerical evaluation of (29) and (30) is quite tricky, due to oscillating and slowly decreasing integrands. However, increasing the cutoff wavenumber K_{c} makes the computation easier.

IV. Numerical Results and Conclusion

The GO-SSA model has been applied to the unified directional ocean spectrum [12]. The sea is fully developed, with a wind speed at 15 m/s. EM frequency is in Ku-band, at 14.6 GHz. A monostatic configuration has been chosen, in the plane along the wind. The scattering cross section predicted by GO-SSA is plotted versus the monostatic incidence angle in Fig. 1 for three different values of the cutoff wavenumber: $K_{\mathrm{c}} = K/4, K/8, K/16$, where K is the EM wavenumber. Only copolarized components of the scattered field are shown, VV and HH, and a 10-dB attenuation has been applied to the HH signal to distinguish the two curves around normal incidence. As one can see, the value of the cutoff has the following minor impact on the monostatic diagram: the curves $K_{\mathrm{c}} = K/4$ and $K_{\mathrm{c}} = K/16$ are always closer than 1 dB, except in HH beyond 65°. Note that differences between ocean-spectrum models can induce larger errors. Due to slope modulation, the TSM models give a nonzero cross-polarization in the plane of incidence, which is absent for GO, SPM1, and SSA1 taken separately. These components are discarded, since cross-polarization is a multiple-scattering effect that cannot be handled by combining two single-scattering methods.

The backscattering cross section of Fig. 1 is, following expression (24), the sum of two terms, a damped GO term, GO $\times\, e^{-Q^2\sigma_{\mathrm{s}}^2}[1-e^{-(q_z\sigma_{\mathrm{L}})^2}]$, and an SSA1 term averaged over large slopes, SSA1 $*$ (pdf slopes). The contribution of each term is shown in Fig. 2 for vertical polarization and three different values of the cutoff. For $K_{\mathrm{c}} = K/4$, the larger term is GO at small angles ($< 20°$) and SSA at larger angles. At smaller cutoffs, $K_{\mathrm{c}} = K/8$, the SSA term dominates everywhere. For $K_{\mathrm{c}} = K/16$, the contribution of the GO term at nadir is as low as 0.2 dB.

Fig. 3 shows a comparison of GO-SSA with GO-SPM at various values of the cutoff $(K_{\mathrm{c}} = K/16, K/8, K/3)$. The

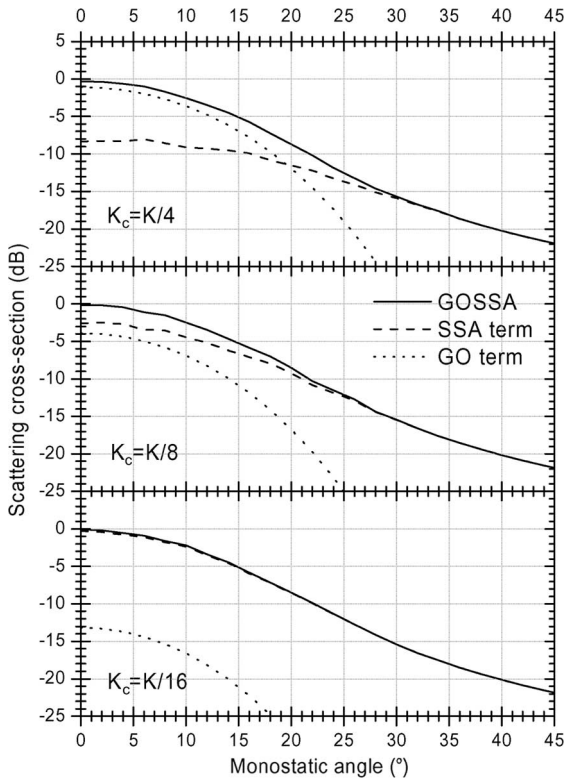

Fig. 2. Contribution of the GO term GO $\times\, e^{-Q^2\sigma_s^2}[1-e^{-(q_z\sigma_L)^2}]$ and of the SSA term SSA1 $*$ (pdf slopes) to the ocean VV backscattering cross section at Ku-band ($f = 14.6$ GHz) versus the monostatic incidence angle, along wind, for a 15-m/s wind speed and for the cutoff wavenumbers $K_c = K/4, K/8, K/16$.

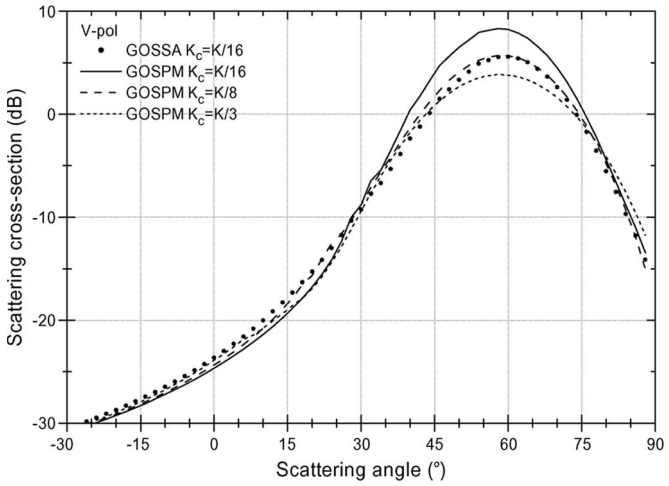

Fig. 3. V-polarized ocean bistatic cross section at L-band ($f = 1.25$ GHz) versus the scattering angle (plane of incidence), along wind, for a 5-m/s wind speed, predicted by GO-SPM for three values of the cutoff wavenumber and GO-SSA.

configuration is bistatic, with an incidence angle of 60° at L-band frequency (1.25 GHz) and for low wind speed (5 m/s). Only the VV component is shown. Due to the damping exponential factor, the diagrams differ around the specular direction, where GO is dominant: here, from 30° to 90°. Replacing SPM1 by SSA1 in the convolution by the pdf of large-scale slopes has also an impact, as it appears on the diagrams between $-30°$ and 30°, where GO-SSA has a larger scattering cross section than GO-SPM regardless of the cutoff. It is interesting to note that the value of the cutoff has a dramatic impact on the level of both GO and SSA taken separately, even though the sum of these two terms remains stable.

To conclude, we have shown in this letter how the principal weakness of the classical TSM for ocean scattering, namely, its dependence on the cutoff, can be amended. The improved model GO-SSA combines two first-order methods, GO and SSA1. The cutoff can be set to nonresonant scales such as $K_c = K/16$, its exact value being unimportant.

ACKNOWLEDGMENT

The authors would like to thank Prof. J. T. Johnson for useful comments on the manuscript and to the anonymous referees for their very constructive remarks. This paper is dedicated to the memory of our friend Tanos Elfouhaily.

REFERENCES

[1] J. W. Wright, "A new model for sea clutter," *IEEE Trans. Antennas Propag.*, vol. AP-16, no. 2, pp. 217–223, Mar. 1968.
[2] G. R. Valenzuela, "Theories for the interaction of electromagnetic and oceanic waves—A review," *Boundary-Layer Meteorol.*, vol. 13, no. 1–4, pp. 61–85, Jan. 1978.
[3] G. Brown, "Backscattering from a Gaussian-distributed perfectly conducting rough surface," *IEEE Trans. Antennas Propag.*, vol. AP-26, no. 3, pp. 472–482, May 1978.
[4] F. G. Bass and I. M. Fuks, *Wave Scattering From Statistically Rough Surfaces*. New York: Pergamon, 1979.
[5] D. R. Thompson, "Calculation of radar backscatter modulations from internal waves," *J. Geophys. Res.*, vol. 93, no. C10, pp. 12 371–12 380, 1988.
[6] J. T. Johnson, R. T. Shinan, J. A. Kong, L. Tsang, and K. Pak, "A numerical study of the composite surface model for ocean backscattering," *IEEE Trans. Geosci. Remote Sens.*, vol. 36, no. 1, pp. 72–83, Jan. 1998.
[7] D. R. Thompson, T. M. Elfouahily, and J. L. Garrison, "An improved geometrical optics model for bistatic GPS scattering from the ocean surface," *IEEE Trans. Geosci. Remote Sens.*, vol. 43, no. 12, pp. 2810–2821, Dec. 2005.
[8] T. Elfouhaily and C. A. Guérin, "A critical survey of approximate scattering wave theories from random rough surfaces," *Waves Random Media*, vol. 14, no. 4, pp. R1–R40, Oct. 2004.
[9] A. G. Voronovich, *Wave Scattering From Rough Surfaces*, ser. Springer Series on Wave Phenomena. Berlin, Germany: Springer-Verlag, 1994.
[10] A. G. Voronovich, "Small-slope approximation for electromagnetic wave scattering at a rough interface of two dielectric half-spaces," *Waves Random Media*, vol. 4, no. 3, pp. 337–367, Jul. 1994.
[11] G. Soriano, C. A. Guérin, and M. Saillard, "Scattering by two-dimensional rough surfaces: Comparison between the method of moments, Kirchhoff and small-slope approximations," *Waves Random Media*, vol. 12, no. 1, pp. 63–88, Jan. 2002.
[12] T. Elfouhaily, B. Chapron, K. Katsaros, and D. Vandemark, "A unified directional spectrum for long and short wind-driven waves," *J. Geophys. Res.*, vol. 102, no. C7, pp. 15 781–15 796, Jul. 1997.
[13] S. T. McDaniel, "Diffractive corrections to the high-frequency Kirchhoff approximation," *J. Acoust. Soc. Amer.*, vol. 79, no. 4, pp. 952–957, Apr. 1986.
[14] J. C. Novarini and J. W. Caruthers, "The partition wavenumber in acoustic backscattering from a two-scale rough surface described by a power-law spectrum," *IEEE J. Ocean. Eng.*, vol. 19, no. 2, pp. 200–207, Apr. 1994.
[15] B. Chapron, K. Katsaros, T. Elfouhaily, and D. Vandemark, "A note on relationships between sea surface roughness and altimeter backscatter," in *Proc. Sel. Papers 3rd Int. Symp. Air-Water Gas Transf.*, 1995, pp. 869–878.
[16] C. A. Guérin and A. Sentenac, "Second-order perturbation theory for scattering from heterogeneous rough surfaces," *J. Opt. Soc. Amer. A, Opt. Image Sci.*, vol. 21, no. 7, pp. 1251–1260, Jul. 2004.